

60.18, H 5.68, N 4.39. Obsd: C 59.99, H 5.82, N 4.19.

Preparation of Films. Polymer 1 was dissolved in a solution of acetone/THF (1:1). The solution was filtered and then cast on a clean level glass surface in a dust-free drybox. The solution was then covered to slow the rate of solvent evaporation. After 48 h, the films were removed from the glass and were vacuum dried for 24 h. The films were soaked and sonicated in deionized water, ethanol, and then hexane before storage in a sealed bottle.

Surface Reactions of 1. Solutions of reagents a-f were prepared by cooling the undiluted alcohol (30 mL) in an ice bath and adding sodium (0.8 g). The reaction mixture was stirred for 24 h or until all the sodium had reacted. Bu_4NBr (1.0 g) was then added. Films of 1 were immersed in the solutions of a-c for 12 h at 100 °C, and in solutions d-f for 3 h at 70 °C. The films were removed from the reaction medium and were rinsed and then soaked in deionized water.

Solution Reactions. Polymer 1 (1.0 g) was dissolved in dry THF (50 mL). Sodium (0.25 g) was added to undiluted 2-(2-aminoethoxy)ethanol at 0 °C. The reaction mixture was stirred

overnight at room temperature or until all the sodium had reacted. $n\text{-Bu}_4\text{NBr}$ (0.5 g) was then added to the salt solution. The alkoxide solution was added slowly to the polymer solution, and the mixture was stirred for 24 h at 70 °C. The reaction mixture was concentrated on the rotary evaporator and then dialyzed (M_w cutoff = 10 000-12 000) against deionized water for 4 days and against methanol for 3 days. The polymer was isolated by evaporation of the contents of the dialysis tube.

Treatment of the Modified Surfaces with Phenyl Isocyanate. Untreated and reacted films of 1 were immersed in 10 mL of a 4% (v/v) solution of phenyl isocyanate in ether at room temperature for 2 h. The films were removed and were washed with and soaked in diethyl ether for 4 h. They were then rinsed and soaked in ethanol and deionized water. Finally, the films were vacuum dried for 24 h.

Acknowledgment. This work was funded by the National Institutes of Health through the National Heart, Lung, and Blood Institute (Grant No. HL 11418).

Photoconductor Fatigue. 1. Photochemistry of Hydrazone-Based Hole-Transport Molecules in Organic Layered Photoconductors: Spectroscopic Characterization and Effect on Electrical Properties

J. Pacansky,* R. J. Waltman, R. Grygier, and R. Cox

IBM Almaden Research Center, 650 Harry Road, San Jose, California 95120-6099

Received November 8, 1990. Revised Manuscript Received March 1, 1991

The hole transport molecule *p*-(diethylamino)benzaldehyde diphenylhydrazone (DEH) undergoes a photochemical reaction to an indazole derivative when exposed to light with $\lambda \leq \sim 480$ nm. When contained in the hole-transport layer of an organic photoconductor formulation, a clear and direct relation is found between the DEH photochemistry and an increase in the residual surface voltage during light decay of the organic photoconductor. Spectroscopic data and electrical properties measurements with DEH and its derivatives firmly establish this correlation. The increase in residual surface voltage is attributed to the trapping of holes in the charge-transport layer during light decay.

Introduction

Electrophotography is the process by which an electrostatic image, formed on the surface of a photoconductor, is transferred and developed on paper by using a toner containing, for example, carbon black.¹ A typical electrophotographic process used in commercial copiers and printers is illustrated in Figure 1. A layered organic photoconductor (to be described below) is wrapped around a drum and, at step (a) in the dark, the photoconductor is charged by a negative corona to about 900 V; this latter quantity is referred to as the dark voltage. During the time required for the photoconductor drum to move from the charging station (a) to the discharge station (b) the electrical conductivity of the photoconductor must be low enough so that the surface potential changes negligibly with time; this decrease in dark voltage with time is commonly labeled dark decay. At step (b) areas of the charged photoconductor are selectively exposed to light and in these exposed regions the photoinduced current ultimately erases the surface charges, leaving on the surface of the photoconductor a latent electrostatic image; the drop in voltage, referred to as light decay, must be rapid and must return as close as possible to zero. The residual voltage

after exposure is often called the white voltage. At the center of Figure 1 the relevant changes in electrical properties that the photoconductor exhibits are plotted as a function of time from station to station. This, of course, is the photoinduced discharge curve and represents ideal photoconductor behavior.

The electrostatic image is developed into a real image on paper by using negatively charged carbon black particles; this development process is shown in Figure 1c, where the toner (containing charged carbon particles) is brought into contact with the photoconductor by using magnetic carrier beads that are charged positively. During the development stage the negatively charged carbon black toner particles move to the exposed regions of the photoconductor due to the lower surface potential. At Figure 1d the carbon black is transferred to paper and heated to fuse the image. The process is now complete and the drum returns to (a) to repeat the process, all of which occurs several times or more a second; the cycle occurs about 10^3 - 10^6 during the lifetime of the photoconductor.

It is clear from Figure 1 that the photoconductor is subjected to light and corona discharges. Additional environmental stresses that the photoconductor is subjected to that are not obvious from Figure 1 are heat (primarily generated by the heat required to fuse toner to paper), and light from fluorescent lights in the work environment (room light). Although, the accumulative incident dose

(1) Carlson, C. *Xerography and Related Processes*; Dessauer, J. H., Clark, H., Eds.; The Focal Press: New York, 1965; pp 15-49.

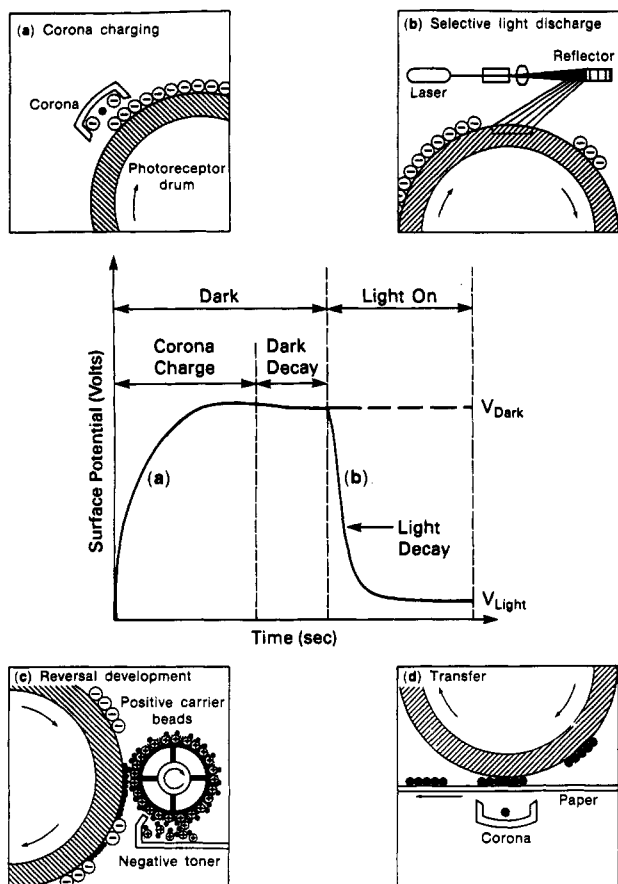


Figure 1. Photoinduced discharge curve related to various points in the electrophotographic process.

received from room light and light used to discharge the photoconductor both appear to be minor, of the order of 1 J/cm^2 ; nevertheless, the photocurrents generated during the discharge process are also very small and subject to significant changes if the incident dose is translated into photochemical changes. From a different point of view, a photoconductor, in order to have a commercial value, must maintain constant electrical properties for many charge and discharge cycles.² We label the deviations in the photoconductor electrical properties with time as fatigue; electrical fatigue has many sources, as alluded to above, and in addition depends on the particular organic materials used to fabricate the photoconductor. Here and in subsequent reports we study a model photoconductor that clearly exhibits electrical fatigue as a result of photochemistry from room light and discharge light. Light-induced fatigue of the electrical properties of organic layered photoconductors increasingly becomes a major consideration on the lifetime of the photoconductors. Thus light-induced fatigue studies become extremely important, and we have separated it into two main types; room light and discharge light.

In this report, we limit our studies to room light fatigue by investigating the effect of photochemistry of a charge-transport molecule, *p*-(diethylamino)benzaldehyde diphenylhydrazone (DEH), on the electrical properties of an organic layered photoconductor. Thus the photochemical reaction is characterized spectroscopically, and the photoproduct is identified. The presence of the photoproduct in the charge-transport layer (CTL) is correlated to specific changes in the electrical properties of the organic layered photoconductor.

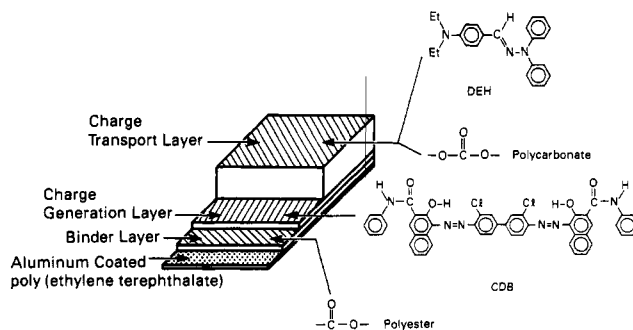


Figure 2. Profile of a layered organic photoconductor.

Structure of the Organic Layered Photoconductor

In the work presented here and in subsequent reports, a model photoconductor is used whose composition and structure are well established. The overall composition of the photoconductor follows those used commercially and thus should serve as a useful test case from which relationships of electrical properties on organic materials may be understood. A brief summary of the structure of the model organic layered photoconductor is presented here; for a more detailed discussion of organic layered photoconductors in general, the interested reader may consult ref 3, for example, or any textbook (e.g., ref 1) on the topic. The organic layered photoconductor, shown in Figure 2, is composed of several key layers. Aluminum coated ($\approx 300 \text{ \AA}$) poly(ethylene terephthalate) serves as a substrate and electrical ground. A binder layer, typically a polyester, is coated atop the aluminized poly(ethylene terephthalate) and serves to adhere the next layer, the charge-generation layer (CGL). The charge-generation layer is composed of an organic dye such as chlorodiane blue (CDB), whose ability to absorb visible light in the presence of a strong electric field is responsible for (light-induced) charge generation. Atop the CGL is the charge-transport layer (CTL), composed of a charge-transport molecule such as the hydrazone DEH, dispersed typically to 40% by weight in a polymeric matrix. While Figure 2 is representative of typical commercial formulations for organic layered photoconductors, a variety of materials may be used as charge-generation and charge-transport molecules. A summary of the types of molecules used by various groups have been given by Nakanishi.⁴

The optical absorption spectrum of the organic layered photoconductor is shown in Figure 3. The charge-transport layer absorbs light $\lambda < \sim 500 \text{ nm}$, which in this case mandates that longer wavelength light must be used to expose the charge-generation layer for carrier generation. Once the absorption characteristics of the photoconductor are known, it is convenient to express the spectral dependence of the light-induced fatigue in more familiar terms; the portion of the light emitted from fluorescent lamps that is absorbed by the CTL lies in the blue region of the visible; henceforth we will refer to the electrical fatigue that results from absorption in this spectral region as "blue light fatigue". The spectral output of discharge lamps used to expose and generate charge in the CGL is in the longer wavelength region of the visible and has a yellow color, and hence electrical fatigue that thus results is referred to as "yellow light fatigue".

Since the charge-transport layer has significant absorption out to $\approx 480 \text{ nm}$ (in the blue region), photochemical changes may occur in the charge-transport layer;

(2) Nguyen, K. C.; Weiss, D. S. *Electrophotography* 1988, 27, 2.

(3) Pacansky, J.; Waltman, R. J.; Coufal, H.; Cox, R. *Radiat. Phys. Chem.* 1988, 31, 853.

(4) Nakanishi, K. *Nikkei New Mater.* 1987, 41.

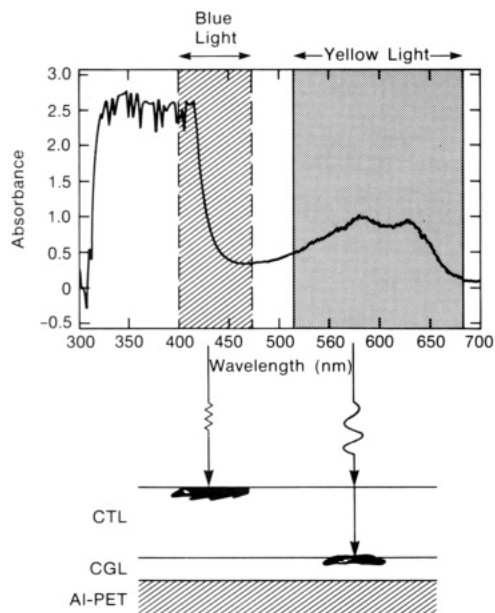


Figure 3. Optical absorption spectrum of an organic layered photoconductor depicted in Figure 2. The intense, broad absorption band between 320 and 450 nm is attributed to the CTL (40% DEH in polymer, 20 μm thick), while the broad bands between 500 and 680 nm are due to the CGL (chlorodiane blue, $\sim 0.1\text{--}0.2\ \mu\text{m}$ thick). Blue light absorption by the CTL (DEH) results in photochemistry at the air/CTL interface, while yellow light absorption by the CGL results in photochemistry initiated at the CGL/CTL interface.

this has indeed been shown to be the case and is a direct result of the high quantum yield for photochemistry exhibited by the charge-transport molecule, DEH,⁵ absorbing light at these wavelengths. The source of the yellow light fatigue, i.e., discharge light fatigue, is caused by absorption of longer wavelength light, $\lambda > 520\ \text{nm}$, by the dye chlorodiane blue at the CGL/CTL interface. This topic will be the subject of another paper.⁶

Experimental Section

DEH and its derivatives were synthesized according to literature procedures.⁷ Chlorodiane blue, polycarbonate, and polyester were obtained from commercial sources. Photoconductors were formulated in the following manner: coating sequentially, a 0.1- μm binder layer of polyester on aluminized poly(ethylene terephthalate) was coated from tetrahydrofuran. The charge-generation layer was next coated, chlorodiane blue from ethylenediamine or hydroxysquarilium/santolite (20%/80% by weight, respectively) to a thickness of 0.2 μm . The charge-transport layer was next coated, 40% by weight of DEH in polymer(s) from tetrahydrofuran to a thickness of 20 μm . Each layer was coated by using the draw coating technique, and each layer was dried before the next was applied.

For light fatigue studies, a fluorescent desk lamp (light source: Inter-World 8CW) with a spectral output $\approx 400\text{--}800\ \text{nm}$ was used. To isolate blue light, the lamp was filtered with Corning CS 4-72 and 7-59 filters in tandem to allow transmission of light between 400 and 480 nm. The incident energies were measured with a United Detector Technology Model 371 optical power meter equipped with a Model 262 head assembly: blue light (incident power = 0.22 mW/cm^2).

The electrical properties of the photoconductors were investigated by using a rotating disk electrometer; a full account of the rotating disk electrometer has been given in a recent publication.³ To investigate electrical fatigue effects, the organic

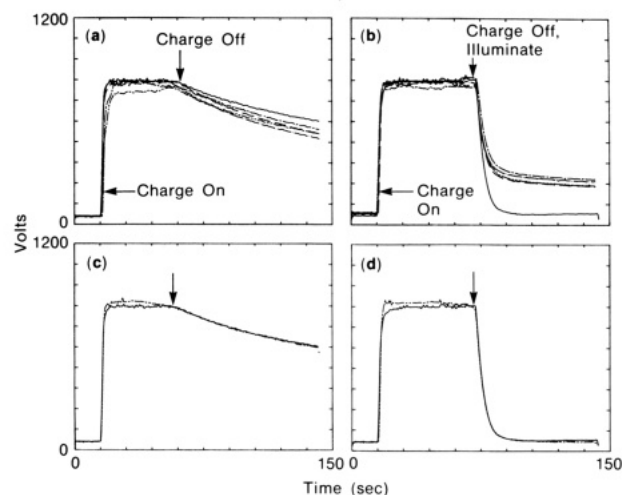


Figure 4. (a) Dark and (b) light decay curves for an organic photoconductor with a CTL derived from 40% by weight of DEH in polycarbonate as a function of blue light exposure (0.22 mW/cm^2 ; 400–480 nm): 0 (—); 0.8 (---); 2.4 (-.-.); 4.0 (·-·); and 15.8 J/cm^2 (---). (c) and (d) compare the dark and light decay curves of the electrically fatigued (15.8 J/cm^2) photoconductor after annealing (---) at $T = 60\ ^\circ\text{C}$ for 1 h, with the virgin dark and light decay curves (—), respectively.

photoconductors were exposed to blue light in air, at room temperature, and their electrical properties immediately measured on the rotating disk electrometer. The blue-light-exposed photoconductor samples were not allowed to stand for any length of time greater than several minutes before electrical measurements were made because partial recovery of their initial electrical properties could occur if the photoconductor samples were left standing (in the dark) for several hours or more; annealing above the glass transition temperature accelerated this recovery, as will be discussed.

For transmission optical absorption studies of DEH photochemistry, a charge-transport layer of 40% by weight of DEH (and its derivatives) in polycarbonate was spin coated onto quartz substrates from tetrahydrofuran solvent and dried (in the dark) under vacuum at 50 $^\circ\text{C}$ prior to use. For emission and attenuated total reflection (ATR) infrared studies, both photoconductor and charge-transport layer films on substrates were used, as described above. The electronic absorption spectroscopy was followed by using an IBM Instruments 9430 UV-visible spectrophotometer. The emission from the organic layered photoconductor was recorded on a Varian SF-330 spectrofluorometer. A JASCO FP-2020 solid sample holder was used to mount the photoconductor sample. The exciting wavelength was maintained at 360 nm and the angle of incidence was 30 $^\circ$ from normal. The infrared spectra were recorded on a Perkin-Elmer 580 spectrometer. An ATR adapter, manufactured by Perkin-Elmer (Model No. 0186-0382), was used for the photochemical and thermal diffusion experiments. KRS-5 plates, set at a 45 $^\circ$ angle, were used in the ATR unit; the dimensions of the plates are 52 \times 18 \times 2 mm^3 .

Results and Discussion

Changes in Electrical Properties. The dark and light decay curves for an organic photoconductor formulated by using a charge transport layer (CTL) of 40% by weight of DEH in polycarbonate atop a charge-generation layer (CGL) of chlorodiane blue, are shown in Figure 4. Before exposure of the CTL to "blue light", $\lambda = 400\text{--}480\ \text{nm}$, the dark decay curve is observed to hold charge and the corresponding photodischarge results in no residual surface voltage. As the organic layered photoconductor is exposed to blue light, resulting in photochemistry of the hole-transport molecule DEH in the charge transport layer, the most significant change observed in the electrical properties of the photoconductor is the evolution of residual surface charges during light decay (Figure 4b). The onset of residual surface charges is rapid, requiring just less than

(5) Pacansky, J.; Coufal, H.; Waltman, R. J.; Cox, R.; Chen, H. *Radiat. Phys. Chem.* **1987**, *29*, 219.

(6) Pacansky, J.; Waltman, R. J., manuscript in preparation.

(7) Arita, T.; Mabuchi, M.; Umehara, S.; Sakai, K. *Ger. Offen. DE 3,331,259*, 1984.

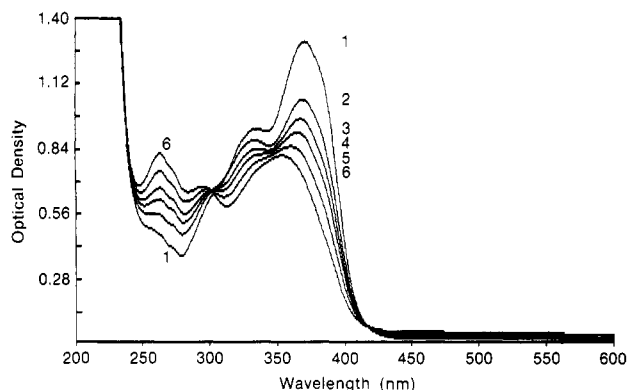


Figure 5. Optical absorption spectrum of 40% by weight of DEH in polycarbonate as a function of blue light (10.9 mW/cm^2 ; $\lambda = 400\text{--}480 \text{ nm}$): Traces 1–6 are 0, 3.3, 6.5, 9.8, 16.4, and 26.2 J/cm^2 , respectively.

1 J/cm^2 to develop several hundred volts, and further exposure to blue light reveals only modest increases in residual surface charges. Thus the organic layered photoconductor fails to photodischarge as a result of the DEH photochemistry in the CTL. The residual charges remain for several tens of minutes even in the presence of the photodischarge lamp, much slower than the normal photodischarge event that would take place in several milliseconds if not for DEH photochemistry. The photochemistry of DEH therefore produces a high background image, completely unacceptable in electrophotographic applications. We coin the acronym "blue light fatigue" to characterize this behavior. Conversely, the dark electrical properties are observed to change little after blue light exposure, with just a modest decrease in dark charge acceptance after 16 J/cm^2 and virtually no change in dark decay rates. Interestingly, the initial electrical properties of the photoconductor may be recovered in the short term by annealing the organic layered photoconductor at a temperature close to its glass transition (Figure 4c,d); the number of "recoveries" is finite and is attributable to irreversible photochemical damage of DEH. This will be explained in greater detail below.

Photoproduct from DEH Photochemistry. To elucidate the cause of blue light fatigue on the electrical properties of organic layered photoconductors, the changes in the electrical properties must be correlated with physical and/or chemical changes in the photoconductor. Thus several spectroscopic methods of analysis were employed to corroborate the changes in the electrical properties, in an effort to understand the origin of blue-light-induced electrical fatigue.

Electronic Absorption Spectra. To monitor the effect of blue light on the electronic absorption spectrum of the CTL more readily, a thin film ($0.3 \mu\text{m}$) of 40% by weight of DEH in polycarbonate was coated onto a quartz substrate and irradiated with the filtered light of a fluorescent lamp to allow transmission of light of $\lambda = 400\text{--}480 \text{ nm}$. These data are shown in Figure 5. Trace 1 is the spectrum of DEH in polycarbonate before irradiation with blue light. The band maximum at 368 nm is attributed to the hydrazone DEH; polycarbonate absorption begins at $\lambda < \sim 250 \text{ nm}$. Several changes in the optical absorption spectrum are apparent upon exposure to blue light: There are (1) a decrease in the band maximum at 368 nm that coincides with the growth of a new band at 265 nm and (2) an isosbestic point at 300 nm indicative of (primarily) a single photoproduct. We have isolated the majority photoproduct and characterized it via standard spectroscopic methods and X-ray structure analysis; these data reveal it to be 1-phenyl-3-(4-(diethylamino)-1-phenyl)-

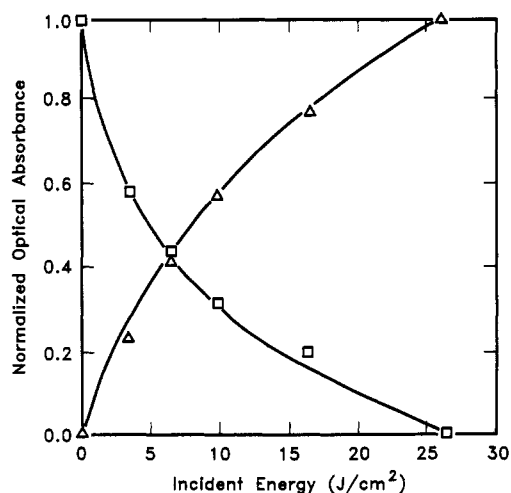
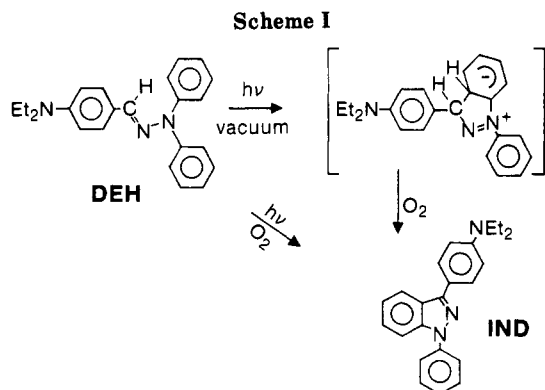


Figure 6. Normalized decay in the band maximum of DEH (368 nm) and the increase in absorption of the indazole derivative (265 nm) as a function of incident blue light; note the decay of DEH is correlated with the formation of the indazole derivative. For the indazole derivative, we have plotted N/N_{max} , where N_{max} is the maximum optical density of the 265-nm band.

1,3-indazole, an indazole derivative hereafter referred to as IND.⁸ Thus DEH in polycarbonate, in the presence of air and blue light, undergoes a photocyclization reaction as shown in Scheme I.

A comparison of trace 6 in Figure 5 to the optical absorption spectrum of authentic IND⁵ corroborates its identification. Thus after an incident dose of $\sim 20\text{--}30 \text{ J/cm}^2$, most of the DEH in the polycarbonate-based CTL has been photochemically converted to the indazole derivative. Figure 6, a replot of Figure 5, shows that the decay in the optical density of DEH is kinetically correlated to the increase in the optical density of the indazole derivative.

To explore whether any of the absorptions are temperature dependent and thus form a basis for a thermally reversible photochemical change, films were heated to temperatures just above the glass transition temperature T_g of the DEH/polycarbonate CTL, i.e., 57°C after they were exposed to light for 3 and 15 J/cm^2 , respectively; however, no changes in the optical absorption spectra were observed. In fact, heating of a larger number of irradiated films did not cause any changes in the electronic or infrared absorption spectra obtained in a *transmission* mode. Thus the photochemical conversion of DEH to an indazole derivative by blue light is conclusive.

From the optical absorption studies contained in Figures 5 and 6, and the electrical properties measurements shown in Figure 4, it is possible to correlate the extent of DEH photochemistry in the CTL with evolution of residual voltage on the organic photoconductor, and such a plot is

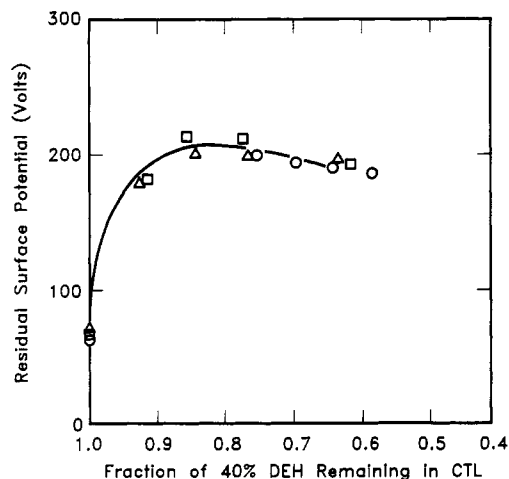


Figure 7. Evolution of residual surface potential on the photoconductor as a function of fraction of DEH remaining in the charge transport layer. The initial concentration of DEH in the CTL is 40% by weight in polycarbonate.

summarized in Figure 7 for three separate photoconductor samples. These data clearly illustrate that significant residual voltage is observed with the photoconductor samples after $\approx 10\%$ of the DEH in the charge-transport layer is photochemically converted. A comparison of Figures 4 and 6 reveals that a residual surface potential of several hundred volts is attained after $\sim 1 \text{ J/cm}^2$ is incident on the photoconductor, which from Figure 6 corresponds to $\sim 15\text{--}20\%$ photochemical conversion of the hole-transport molecule DEH to photoproducts. Since the indazole derivative is the primary photoproduct,⁸ we conclude that its formation in the charge-transport layer is associated with the residual voltage evolution.

Evidence for Accumulation of the Indazole Derivative and Recovery of Initial Electrical Properties. The recovery of the initial electrical properties of the fatigued photoconductor after annealing or left standing is an issue that has remained little understood.² In support of the model proposed above, we have performed experiments that demonstrate that the accumulation of the photoproduct, an indazole derivative, near the surface of the charge-transport layer (CTL), its diffusion, and subsequent redistribution in the bulk of the CTL is important for the recovery of the initial electrical properties. To investigate these aspects, spectroscopic techniques that are sensitive to the CTL/air interface are necessary to observe diffusion effects which would otherwise be absent utilizing *transmission* spectroscopy, since diffusion (within a film) causes no net changes in concentration of chemical species, only in their distribution across a film.

Emission Spectra. Organic layered photoconductor samples were placed in a spectrofluorometer, and the emission spectra recorded as a function of exposure time and thermal treatment. The exciting wavelength was set at 360 nm, and the emission was spectrally analyzed from 400 to 600 nm. For reference, the emission spectra of authentic DEH and of the indazole derivative in the CTL polymeric binder (40% by weight in binder) are respectively shown in Figure 8. The emission from DEH has its maximum peak intensity at 470 nm, whereas the indazole derivative (IND) shows a peak at 413 nm and a shoulder at 450 nm. In Figure 9, a set of emission spectra are shown for the organic layered photoconductor as a function of exposure time under the filtered desk lamp. Since the exciting wavelength is 360 nm, only a relatively

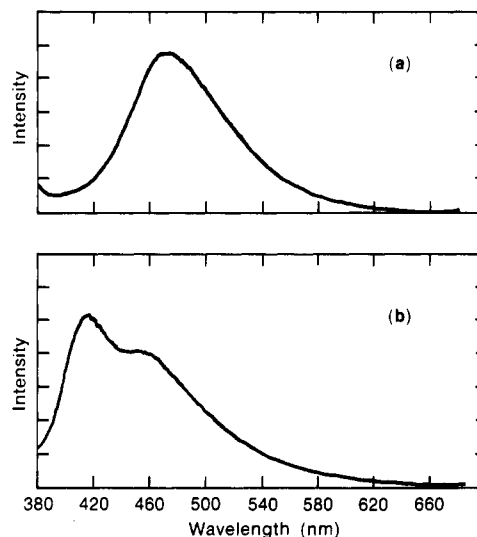


Figure 8. Emission spectra from 360-nm excitation of (a) 40% DEH in polycarbonate and (b) 40% indazole derivative in polycarbonate. The maximum peak intensity occurs at 470 nm for DEH and 413 nm for the indazole derivative. Both films were $\sim 2 \mu\text{m}$ thick.

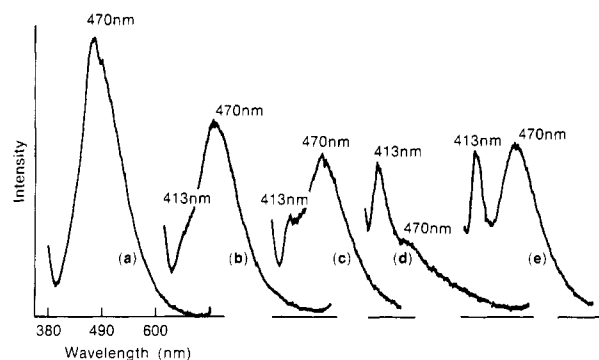


Figure 9. Emission spectrum from 360-nm excitation of a DEH-derived organic photoconductor as a function of incident energy from blue light exposure (0.2 mW/cm^2) prior to recording the emission spectrum: (a) 0; (b) 1.3; (c) 3.2; (d) 13.6 J/cm^2 ; (e) anneal sample (d) for 4 h at 80°C . The maximum at 470 nm (DEH) is gradually converted to another maximum at 413 nm (indazole derivative). Annealing of the sample "recovers" the DEH emission due to refreshing of the charge-transport layer surface with DEH via diffusion.

thin part of the CTL close to the surface of the film is interrogated (discussed later in Figure 11). The spectra shown in Figure 9, however, indicate that as a function of exposure the emission spectrum of DEH is being converted to the emission spectrum of the indazole derivative. Consequently, emission spectroscopy corroborates the conclusions derived from the electronic absorption spectroscopy, that is, the photoconversion of DEH to an indazole derivative and, additionally, that the indazole derivative is present near the surface of the charge transport layer.

In Figure 10 the results of the electronic emission spectra are replotted. This figure shows that the decay in the emission of DEH is kinetically correlated to the increase in emission of the indazole derivative, consistent with the optical absorption studies discussed in Figure 6.

The last spectrum in Figure 9, obtained after the exposed sample was heated, reveals a temperature dependence. After heating to 80°C for 4 h, the intensity of the DEH emission is detected again. When the sample is cycled through a blue light exposure and an annealing step, the DEH emission returns, but to a lower initial value at the start of each cycle, and the emission from the indazole

(8) Pacansky, J.; Coufal, H.; Brown, D. W. *J. Photochem.* 1987, 37, 293.

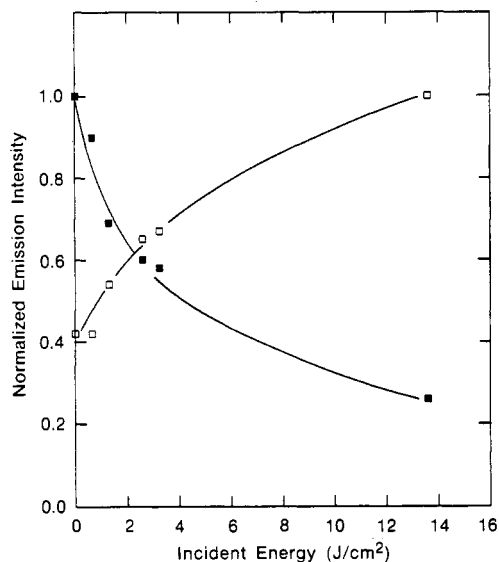


Figure 10. Normalized emission intensity of DEH (470 nm) and indazole derivative (413 nm) as a function of incident energy from the blue light of the filtered fluorescent lamp (400–480 nm; 0.2 mW/cm²).

derivative steadily gains intensity. It will be recalled from Figure 5, which showed the electronic absorption spectrum of DEH as a function of blue light, that heating the film after photochemical conversion to the indazole derivative produced no changes in the spectrum in the *transmission* mode. We explain the temperature dependence of the emission spectrum on a diffusion process that is accelerated when we heat to and above the $T_g = 57^\circ\text{C}$ of the CTL, which redistributes the DEH and indazole derivative in the charge transport layer. This is supported by the ATR measurements in the next section.

ATR Spectroscopy. Attenuated total reflection (ATR) infrared spectroscopy was used to analyze the changes occurring in a thin layer close to the surface of the charge-transport layer (CTL). Samples of the photoconductor were exposed to blue light (400–480 nm) as a function of exposure time and heated as before. The ATR spectrum of an unexposed photoconductor sample is shown in Figure 11a where two DEH bands centered at 1525 and 1495 cm^{-1} are identified. Figure 11b contains the ATR spectrum after exposure for 20 J/cm²; Figure 11c exhibits the spectrum recorded after heating the same sample to 100 °C for 1 h; and Figure 11d contains the ATR spectrum of neat DEH for comparison. The IR absorption at 1525 and 1495 cm^{-1} are characteristic for DEH and has been discussed in connection with the photochemistry of DEH.⁸ These absorptions and all of the other absorptions due to DEH synchronously decrease in intensity with an increase in intensity of the indazole derivative. After annealing the sample at $T = 100^\circ\text{C}$ for 1 h, the 1525- and 1495- cm^{-1} features regain intensity like that observed for the emission spectrum. We note that spectra recorded via transmission infrared do not show the temperature-reversible behavior for DEH or the indazole derivative.

The absorption of blue light by DEH in a polymer binder may be modeled. Simmons⁹ has derived an analytical solution that describes the rate of photochemical reaction of a solid layer which gives rise to a transparent photoproduct. The DEH photoconversion to the indazole derivative is approximately such a case due to the shift in the band maximum from 368 nm for DEH to 350 nm for the indazole derivative, as discussed in Figure 5. Thus,

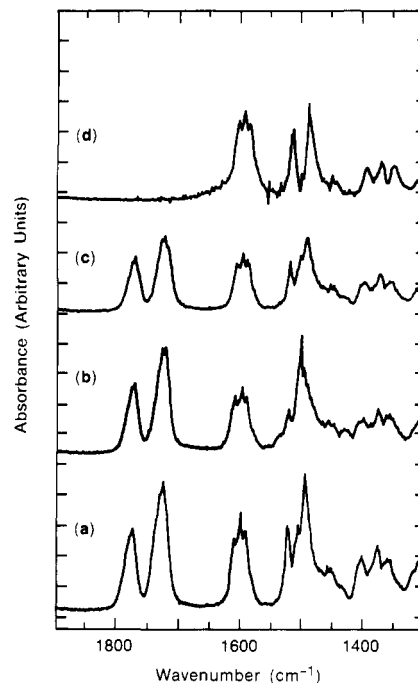


Figure 11. ATR spectrum of a DEH-based organic photoconductor (a) before exposure to blue light, (b) after 20 J/cm² exposure to blue light, (c) anneal sample shown in (b) for 1 h at 100 °C, and (d) thin film of DEH.

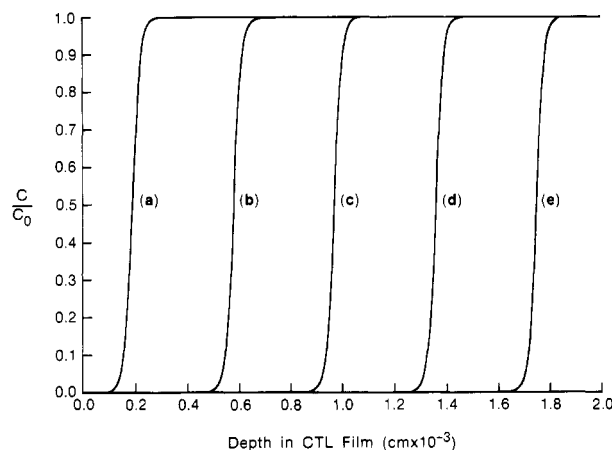


Figure 12. Model for the concentration profile in a DEH-based charge-transport layer as a function of depth into the film, for the photochemical conversion of DEH to an indazole derivative. For the model, the concentration of DEH is 40% by weight in a polymer, the exposure achieved by monochromatic radiation ($\lambda = 400\text{ nm}$) with a quantum yield for photochemistry of $\phi = 0.4$ (for DEH). The exposure times are (a) 1000, (b) 3000, (c) 5000, (d) 7000, and (e) 9000 s.

if DEH is irradiated at $\lambda \approx 400\text{ nm}$, then indazole absorption at that wavelength is negligible. Thus starting with the following equation:

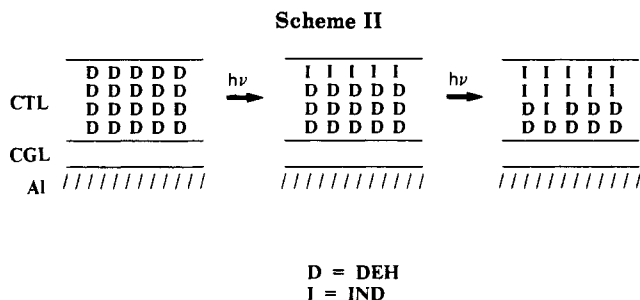
$$dC/dt = -\phi\alpha CI \quad (1)$$

where I = light intensity (einsteins/cm² s), C = concentration (mol/cm³), x = depth into film, t = time, α = absorption coefficient, and ϕ = quantum efficiency of photoreaction, the analytical solutions are

$$\frac{C}{C_0} = \frac{e^{-\phi\alpha I_0 x}}{e^{-\phi\alpha I_0 t} \{1 - e^{-\alpha C_0 x}\} + e^{-\alpha C_0 x}} \quad (2)$$

Figure 12 illustrates the reactant concentration C/C_0 profile across a solid film, for 40% DEH in a polymer, using $\phi = 0.4$ as determined experimentally for the pho-

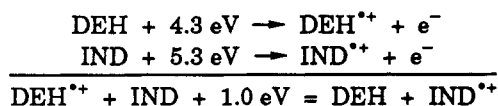
(9) Simmons, E. L. *J. Phys. Chem.* 1971, 73, 588.



to-reaction of DEH to the indazole derivative.⁵ The formation of the indazole derivative from DEH is evident from the series of curves generated for the concentration gradient. At time $t = 0$ s, the film is entirely DEH (in polymer). As the irradiation time is increased to $t = 1000$ s, DEH is depleted near the surface of the charge-transport layer, and the trend continues as a function of irradiation. Since the rate of photochemical conversion is much greater than rate of diffusion of photoproduct in the polymer binder, under these conditions, the concentration profile is fairly uniform across the DEH/polymer film and, thus, the photoreaction at short times is essentially surface localized with very little redistribution of products in the polymeric binder. Thus a layer of the indazole derivative is formed in the CTL. We note that the use of eq 2 is valid for monochromatic radiation only; for modeling purposes, a λ of 400 nm was used. For the optical absorption studies outlined in Figure 5, polychromatic radiation was used with $\lambda \approx 400\text{--}480$ nm; hence no attempt to fit the experimental data to the modeling is provided. The modeling is presented merely to corroborate the experimental results and to illustrate that the initial photochemistry is essentially surface localized; the longer wavelength contribution in the actual experiment will serve to cause deeper penetration of blue light into the film. The accumulation of the indazole derivative in the charge-transport layer (CTL) has severe consequences on the electrical properties of an organic layered photoconductor as a function of irradiation, as will be discussed shortly.

In blue light fatigue, the appearance of the indazole derivative coincides with changes in the electrical properties of the photoconductor and thus is considered to be primarily responsible for the electrical fatigue of the type observed in Figure 4b. This photochemically induced change in the CTL is considered in Scheme II. As outlined in the modeling for the concentration profile (Figure 12), photoproducts are initially accumulated at or near the surface of the charge transport layer. Thus, as the indazole derivative I is formed from DEH D in the CTL, a heterogeneous layer is created in the charge-transport layer composed of a DEH/indazole derivative interface.

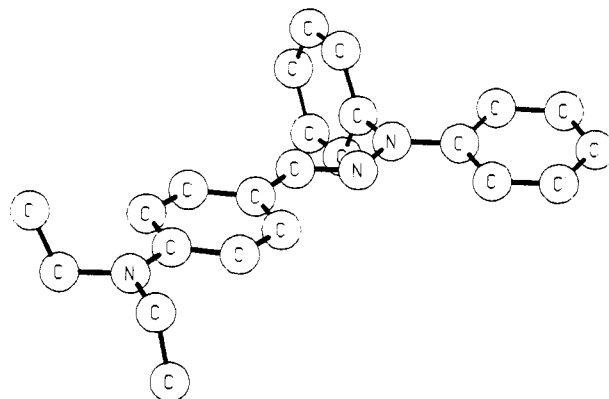
The origin for the lack of hole transport through an IND layer may be immediately deduced from XPS data by using the solid-state vertical ionization potential of DEH (4.3 eV) and IND (5.3 eV).⁶



For DEH to inject a hole into the indazole derivative IND, energy is required. Consequently a barrier to hole injection from DEH to IND exists that is electric field driven; the smaller the externally applied electric field, the more difficult it is for the hole DEH^{++} to overcome the energy barrier and inject the hole into IND, the indazole derivative. Thus in the photodischarge curves shown in Figure 4b, while light decay at high fields is not impeded by the

presence of IND in the CTL, at low fields hole injection efficiency decreases appreciably. We note here that a photoconductor formulation using 40% IND in polycarbonate as the hole-transporting molecule does in fact photodischarge;¹⁰ therefore, the origin of the hole trapping in the charge-transport layer containing a DEH/IND interface is attributed to the trapping of holes on DEH at the DEH/IND interface, in the limit of a low externally applied electric field. A detailed report on the energetics of the hole trapping will be published shortly.⁶

Inhibition of the Photocyclization Reaction. The photocyclization reaction of DEH to the indazole derivative plays a significant role in propagating electrical fatigue. A chemical remedy for the photocyclization reaction is to alter the structure of DEH so that the photocyclization reaction may be inhibited and, simultaneously, retain its excellent transport and processing properties. Since this is a structural optimization problem, it is instructive to first understand the molecular structure of DEH itself. An X-ray crystal structure analysis has shown that the DEH molecule is essentially composed of two separate entities, a substituted aniline and a substituted hydrazone, sharing a common π -system. The π -system is extended, ranging from the amine nitrogen atom of the diethylaniline portion of the molecule, to the amine nitrogen atom of the diphenylhydrazone moiety. One of the phenyl groups on the diphenylhydrazone portion of the molecule lies coplanar to the extended π -system, and the other is nearly perpendicular to it.⁸ This is illustrated as



It has been proposed⁸ that the portion of the molecule in DEH which gives rise to the photocyclization reaction is the diphenylhydrazone portion and, in particular, the phenyl ring that is perpendicular to the π -system; the reaction pathway has been illustrated in a previous scheme. Thus photocyclization involves a ring closure of the ortho-carbon atom of the perpendicular phenyl ring with the benzaldehyde carbon atom, followed by loss of two hydrogens in the presence of blue light and oxygen. It is therefore possible that substitution of the ortho position of the perpendicular phenyl ring of diphenylhydrazone with a substituent may retard the photocyclization reaction. Alternatively, the H atom on the carbon atom adjacent to the imine may also be replaced by a methyl group. As an example, let us consider the former solution. Thus a methyl substituent on the ortho position of the perpendicular phenyl group, attached to the hydrazone amine, may sterically inhibit the ring closure and thus may retard photocyclization. To test this hypothesis, a single methyl substituent was placed at an ortho position of one of the phenyl rings in the diphenylhydrazone portion of the

(10) *Research Disclosure*, 1990, 318, Number 31872 (disclosed anonymously).

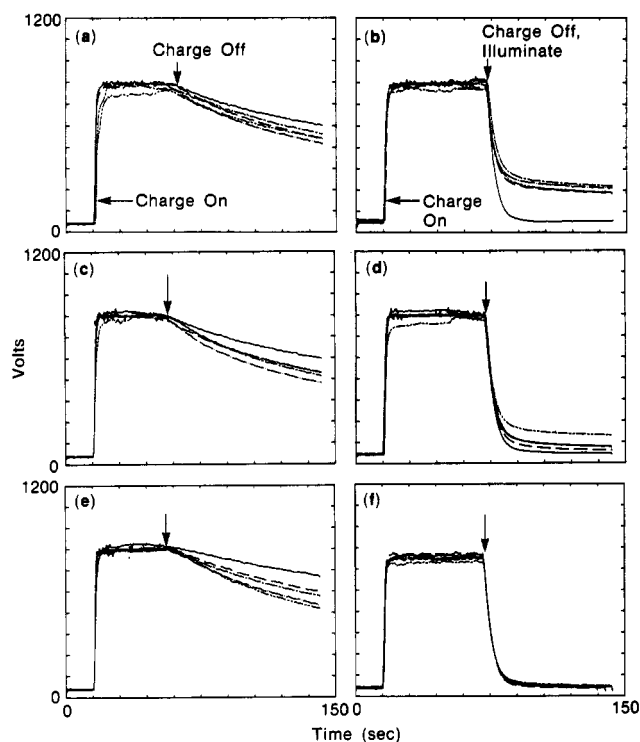
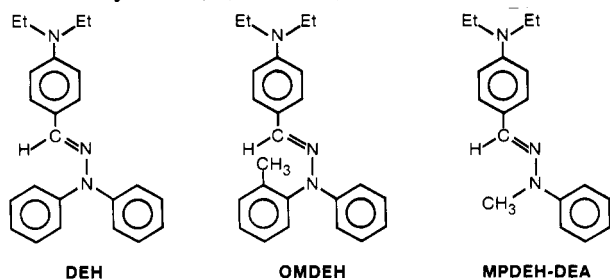


Figure 13. Dark and light decay curves for an organic photoconductor with a CTL derived from: (a) and (b) 40% by weight DEH in polycarbonate; (c) and (d) 40% by weight OMDEH in polycarbonate; (e) and (f) 40% by weight MPDEH-DEA in polycarbonate as a function of blue light exposure (0.22 mW/cm^2 ; $400\text{--}480 \text{ nm}$): 0 (—); 0.8 (---); 2.4 (---); 4.0 (---); and 15.8 J/cm^2 (---).

molecule. A subsequent crystal structure analysis has revealed that the substituted phenyl ring prefers to be perpendicular to the π -system. The chemical structure⁶ of "o-methyl DEH" (OMDEH) is shown as follows:



OMDEH was therefore formulated into the standard polymeric binder, and its electrical properties were tested in the usual manner; the results are illustrated in Figure 13. As expected, evolution of residual charge as a function of blue light exposure is significantly retarded. After an incident exposure of 1 J/cm^2 , modest residual charge above "background" is observed for the OMDEH-based charge-transport layer, whereas for a formulation with DEH, significant residual charge is evident after only 1 J/cm^2 . The evolution of residual voltage as a function of incident blue light energy is compared for the various DEH derivatives in Figure 14. Note that when the perpendicular phenyl group is completely removed and replaced by a methyl to avoid the photocyclization reaction, i.e., MPDEH-DEA, there is no residual voltage after comparable exposures to blue light. These data clearly illustrate the correlation between the electrical fatigue of DEH-based organic photoconductors, with DEH photochemistry and indazole derivative formation. Finally, the normalized decay rate of the band maximum in the electronic absorption spectra corroborate these data (Figure 15). A

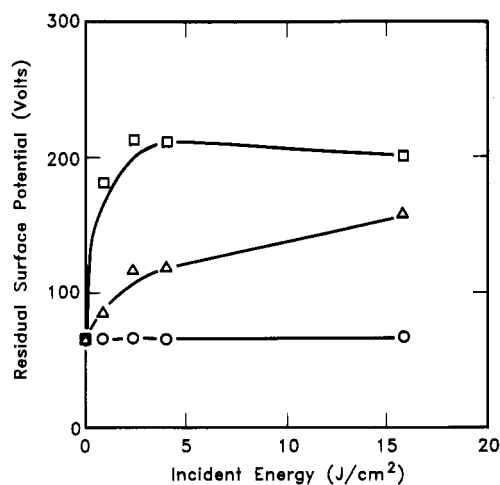


Figure 14. Residual surface potential on photoconductor after exposure to blue light (0.22 mW/cm^2 ; $\lambda = 400\text{--}480 \text{ nm}$) and subsequent photodischarge (light decay). The charge-transport molecules are 40% by weight in polycarbonate: DEH (\square); OMDEH (∇); MPDEH-DEA (\circ).

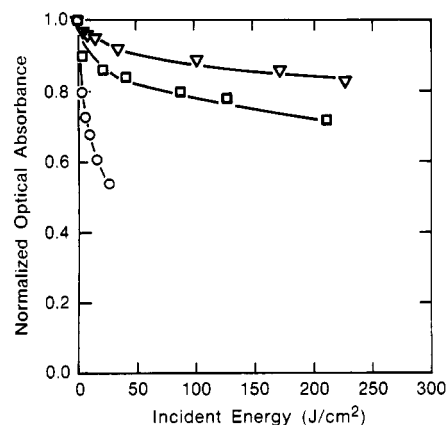


Figure 15. Normalized decay in optical density as a function of incident energy (blue light, 10.9 mW/cm^2 , $\lambda = 400\text{--}480 \text{ nm}$) of the band maximum (370 nm) of DEH, OMDEH and MPDEH-DEA, 40% by weight in polycarbonate films on quartz: DEH (\circ); OMDEH (\square); and MPDEH-DEA (∇).

comparison of their decay rates clearly demonstrate the increasing resistivity to photocyclization in going from DEH to OMDEH to MPDEH-DEA. These data provide conclusive evidence that the photocyclization reaction is responsible for this aspect of blue light fatigue.

Wavelength Dependence of Blue Light Fatigue. In the previous section it was shown that when DEH is exposed to light with $\lambda > 400 \text{ nm}$, all of the DEH in the CTL may be converted to photoproduct. This creates profound changes in the electrical properties of the photoconductor and is possible because the photoproduct does not have any absorption at this long wavelength. However, when DEH is exposed to light with shorter wavelengths, e.g., at its band maximum, $360 \pm 10 \text{ nm}$, (using narrowband filters to isolate the radiation) changes in electrical properties are negligible. We should point out that the quantum yield for DEH photochemistry is not wavelength dependent and that the primary cause for this lack of light induced fatigue is that the photoproduct, IND, has significant absorption in this region. Furthermore, relative to DEH, IND has an extremely small quantum yield for photodecomposition but a very large yield for fluorescence. As a consequence, although DEH is rapidly converted to IND even at this shorter wavelength, once IND is formed it serves as an internal filter and effectively retards any subsequent DEH photochemistry. Thus, in this case the photochemistry is

truly localized at the CTL/air interface resulting in a negligible light-induced fatigue. Electrical conduction through the photoconductor is thus not effected by exposure to the shorter wavelength light, but a very thin film of CTL has its DEH converted to IND. Concomitantly, the electrical conductivity parallel to the surface is effected because IND has a higher oxidation potential; this is an important observation because it directly effects resolution, or in other words the ability to produce hard copies with very small images.

Concluding Remarks and Summary

Electrophotographic processes, used in copiers and printers, place stringent demands on organic photoconductors. Although a photoconductor is subjected to several charge and discharge steps to produce one copy, the cycle is repeated about 10^3 - 10^6 during the normal lifetime of the photoconductor. For the electrophotographic process to operate successfully, the electrical properties, that is, resistivity, conductivity, dark and light voltage, and dark and

light decay, must remain as constant as possible. When this is not the case, the photoconductor is said to suffer "fatigue" and one searches to explain its cause and as a result offer a fix. This task is not at all trivial because one seeks to relate how the flow of very small photocurrents are effected by small physical and/or chemical changes in the organic materials. We present here a model photoconductor with which we have studied the effect of photochemistry using "blue light" on the hole-transporting material, DEH, in the charge-transport layer. A clear and direct relation is found between DEH photochemistry and an increase in residual voltage. To add another layer of validity in support of our conclusions, we synthesized a new DEH derivative that is identical with DEH in every property but has its photochemical activity toward blue light reduced by about 2-3 orders of magnitude. Replacing DEH with this material in the photoconductor in effect eliminates the blue light fatigue and hence firmly establishes a relation between photochemistry and electrical properties.

Design, Synthesis, Characterization, and Use of All-Organic Nonionic Photogenerators of Acid

F. M. Houlihan,* T. X. Neenan,* E. Reichmanis,* J. M. Kometani, and T. Chin†

AT&T Bell Laboratories, 600 Mountain Avenue, Murray Hill, New Jersey 07974

Received November 8, 1990. Revised Manuscript Received March 12, 1991

A study was made of the effects on thermal stability of varying the substitution patterns on 2-nitrobenzyl benzenesulfonate photogenerators of acid. It was found that the thermal stability of these sulfonate esters was dramatically increased by the introduction of an electron withdrawing, sterically bulky group (Br, CF_3) at the ortho position of the benzyl moiety. This enhancement in thermal stability allowed synthetic access to thermally stable photogenerators of acid based on powerful acids such as 2,2,2-trifluoroethanesulfonic acid.

Introduction

In recent years the drive toward smaller feature sizes in the microelectronics industry has led to the development of chemically amplified photoresists. These resists possess an inherently high sensitivity because upon irradiation an initial photonic event generates a catalyst that can then promote a cascade of chemical reactions that completely transforms the irradiated portion of the resist.¹ One type on chemically amplified photoresist depends of the photogeneration of a protic acid.^{2,3}

Until recently, photogeneration of such acids for use in chemically amplified resists required the use of onium salt materials such as triphenylsulfonium hexafluoroarsenate^{2,3} which contained metal atoms. More recently, nonmetallic versions of these onium salts such as diphenyliodonium triflate have been described.⁴ We have previously described the use of 2-nitrobenzyl sulfonate esters as covalent, highly soluble, nonmetallic photogenerators of toxic acid.⁵⁻⁷ Other workers have reported covalent compounds capable of photogenerating nonactivated aryl sulfonic acids,⁸⁻¹¹ methanesulfonic acid,¹² and hydrogen halides.^{13,14} However, these systems all release acids having relatively nucleophilic anions compared with hexafluoroarsenic and

triflic acid, which can be formed by the irradiation of onium salts. This nucleophilicity may limit the catalytic chain lengths of the photogenerated acids and render such acid generators less effective in promoting certain chemical processes such as the catalytic deprotection of poly-

- (1) Willson, C. G.; Frechet, H.; Tessier, J. M. J.; Houlihan, F. M. *J. Electrochem. Soc.* **1986**, *133*(1), 181.
- (2) Ito, H.; Willson, C. G.; Frechet, J. M. J. U.S. Patent 4,491,628, 1985.
- (3) Ito, H.; Willson, C. G.; Frechet, J. M. J. *SPSE Regional Technical Conference on Photopolymers*, Ellenville, New York, Nov 1982.
- (4) Osuch, C.; Brahim, K.; Hopf, F.; Mcfarland, M.; Mooring, A.; Wu, C. *Proc. SPIE* **1986**, *631*, 68.
- (5) Houlihan, F. M.; Shugard, A.; Gooden, R.; Reichmanis, E. *Proc. SPIE* **1988**, *920*, 67.
- (6) Houlihan, F. M.; Shugard, A.; Gooden, R.; Reichmanis, E. *Macromolecules* **1988**, *21*, 2001.
- (7) Neenan, T. X.; Houlihan, F. M.; Reichmanis, E.; Kometani, J. M.; Bachman, B. J.; Thompson, L. F. *Macromolecules* **1990**, *23*, 145.
- (8) Li-Bassi, G. *J. Radiat. Curing* **1987**, *14*(3), 18.
- (9) Berner, G.; Rist, G. *Latent Sulfonic Acids*; Radcure Europe: Basel, Switzerland, 1985; p 446.
- (10) Yamaoka, Y.; Omote, T.; Adachi, H.; Kikuchi, N.; Watanabe, Y.; Shirotsaki, T. *J. Photopolym. Sci. Technol.* **1990**, *3*(3), 275.
- (11) Shirai, M.; Tsunooka, M. *J. Photopolym. Sci. Technol.* **1990**, *3*(3), 301.
- (12) Schlegel, L.; Ueno, T.; Shiraishi, H.; Hayashi, N.; Iwayanagi, T. *Chem. Mater.* **1990**, *2*(3), 300.
- (13) Dossel, K. F.; Huber, H. L.; Oertel, H. *Microelectron. Eng.* **1986**, *986*, 5, 97.
- (14) Menschig, A.; Forchel, A.; Dammel, R.; Lingnau, J.; Scheunemann, U.; Theis, J.; Pongratz, S. *Microelectron. Eng.* **1989**, *9*, 571.

† Barnard College, New York.